Electronic structure of Si nanocrystals codoped with boron and phosphorus

Christophe Delerue

Electronic structure of Si nanocrystals codoped with boron and phosphorus

Christophe Delerue*
Université de Lille, CNRS, Centrale Lille, ISEN, Université de Valenciennes, UMR 8520–IEMN, F-59000 Lille, France

(Received 2 March 2018; revised manuscript received 10 July 2018; published 31 July 2018)

The electronic structure of Si nanocrystals (NCs) doped with B (acceptor) and P (donor) impurities is calculated. A tight-binding approach is employed, allowing us to investigate NCs of up to 10 nm diameter and to compare directly with recent experiments on colloidal Si NCs. The calculations show that the experimental data of optical and electrical spectroscopy are consistent with configurations of full compensation between donors and acceptors. The NC energy gap is narrowed in the presence of codopants and can be even smaller than in bulk Si, but at the same time it varies with NC size under the effect of quantum confinement. Measured energy gaps are compatible with NCs containing a small number (∼2–5) of B-P pairs if we assume a random placement of the dopants in the NC core. B-P clusters in which the B and P atoms are nearest neighbors have a marginal influence on the NC energy gap. In the case of Si NCs doped with a single P impurity, the theory predicts the hyperfine splitting of electron spin resonance as a function of the NC size, in excellent agreement with experiments if the dopant is placed at random positions.

DOI: 10.1103/PhysRevB.98.045434

I. INTRODUCTION

Even though the first report of efficient photoluminescence (PL) from Si nanocrystals (NCs) was published more than 25 years ago [1], the optical properties of Si NCs still receive considerable attention in the context of important developments in Si photonics [2]. New directions of research have greatly benefited from the synthesis of colloidal Si NCs characterized by high structural quality, narrow size distribution, and PL quantum yields sometimes above 60% [3–5]. Other interesting developments came from the synthesis of Si NCs doped with donor (P,As) or acceptor (B) impurities [6–15]. The incorporation of impurities inside the NCs has been clearly demonstrated, in particular using atom probe tomography (APT) analysis [14–18], but the role of these impurities and their electrical doping efficiency remain sources of important debates [19,20]. The situation is quite confusing since, in parallel, several works reported tunable plasmonic properties in highly doped Si NCs prepared by the nonthermal plasma method [21–23].

Donor and acceptor impurities in Si NCs are also interesting for their energy levels in the band gap. It was demonstrated that Si NCs codoped with B and P impurities are characterized by PL emission at lower energy than undoped Si NCs, which is interpreted by optical transitions between energy levels induced by the dopants [24–30]. The codoped Si NCs were first synthesized in borophosphosilicate glass matrices and were subsequently produced in colloidal solutions. These codoped Si NCs combine the advantages of Si NCs, i.e., a size-tunable optical band gap and a relatively high recombination rate (for an indirect gap material), and the effects of the codopants that shift the emission energy to lower values. Remarkably, PL emission below the band gap of bulk Si was demonstrated, which is very appealing to extend the application field of Si NCs to new frequency ranges [28].

The reduction of the optical gap of Si NCs by the B-P codoping is supported by *ab initio* density functional theory (DFT) calculations performed by Ossicini *et al.* [31–34]. The latter have also shown that simultaneous B and P doping strongly reduces the formation energy with respect to both B and P single-doped cases [32]. However, further theoretical investigations are still needed since DFT calculations were limited to NC sizes smaller than in experiments, and NCs doped with more than one B-P pair were not considered. In addition, DFT calculations are known to underestimate the band gap, and calculations based on many-body perturbation theory that go beyond DFT and include excitonic effects could only be performed for NCs containing 35 atoms [32]. For all these reasons, it is still unclear whether the PL emission below the bulk Si band gap can be explained by the influence of the dopants, and important questions remain unresolved. How many active dopants per NC are necessary to explain the redshift of the PL emission? What is the influence of the disorder induced by the varying impurity positions? How can we explain that the optical gap of codoped Si NCs still varies with size, meaning that it is still influenced by quantum confinement effects in spite of the presence of the dopants?

In this paper, I present atomistic tight-binding calculations that address these issues. The methodology, developed to reproduce the donor and acceptor energy levels in bulk Si, describes very well the evolution with size of the hyperfine splitting of the electron spin resonance (ESR) of P-doped Si NCs [8]. This agreement is obtained for electrically active P dopants placed at random positions in the Si NCs. I have calculated the energy gap of codoped Si NCs with diameter up to 10.4 nm and with a number of B-P pairs varying from 1 to 10. I show that an increasing number of B-P pairs tends to enhance the effects of disorder and therefore the variability in the energy gap. However, the mean energy gap

*christophe.delerue@iemn.univ-lille1.fr

decreases for increasing codoping, extending the conclusions of Ossicini *et al.* beyond the single B-P pair case [31–34]. If we assume a random position of the impurities, the experimental data [28] for the PL peak energy and the scanning tunneling spectroscopy (STS) gap [35] versus NC size are compatible with a small number of B-P pairs per NC, below 5 and probably closer to 2. However, the energy gap of the NCs is almost not influenced by B-P atoms in nearest-neighbor configurations. Comparison with experiments shows that the number of electrically active (randomly placed) dopants is much smaller than the number of impurities present in the NCs and their vicinity [17,28].

II. METHODOLOGY

To compare with experiments [28,35], I consider spherical NCs with a diameter up to 10 nm. The NCs are doped with the same number of P and B impurities, i.e., there is a full compensation between donors and acceptors. This is consistent with the assumption that light-emitting Si NCs containing free carriers (electrons in the conduction-band states or holes in the valence-band state) are nonemitting due to efficient Auger recombination [36]. The situation of full compensation may be favored by the small formation energy of B-P pairs compared to single dopants [32]. I assume that the dopants are ideally placed at substitutional sites; surface sites are discarded unless otherwise stated. For each NC size and dopant concentration under investigation, 40 configurations are considered in which the impurity positions are chosen at random, for reasons discussed in the next section. Mean values of the energy gaps are computed by taking the average over the 40 configurations.

The single-particle Hamiltonian of a codoped Si NC is written as

$$H = H_0 + V, \tag{1}$$

where H_0 is the Hamiltonian of undoped Si NC and V is the static potential induced by the impurity nuclei. H_0 is written in a tight-binding framework using the $sp^3d^5s^*$ model of Ref. [37]. The surface of the Si NCs is passivated by hydrogen atoms, each one being described by a single s orbital.

The term V in Eq. (1) describes the potential induced by point charges $\pm e$ positioned at the impurity nuclei where the sign $-$ $(+)$ holds for an acceptor (donor). V is the solution of the Poisson equation in which the system is represented by a sphere of diameter D and of dielectric constant ϵ_{in} embedded in a medium of dielectric constant ϵ_{out}. We use the bulk experimental value $\epsilon_{\text{in}} = 11.7$. This dielectric approach is fully justified when $D \gtrsim 3$ nm [38,39].

The tight-binding treatment of V is straightforward because, as a slowly variable potential, it only appears on the diagonal of the Hamiltonian matrix [38]. The diagonal term at each donor (acceptor) site is considered as a parameter describing central cell effects [40]. The parameters for B and P were determined as described in Refs. [41,42]. This approach gives ionization energies for these impurities in bulk Si in good agreement with the experimental values.

III. DISCUSSION ON THE POSITION OF ELECTRICALLY ACTIVE DOPANTS AND THE DOPING PROBLEM

It has long been accepted that doping of semiconductor NCs is intrinsically difficult, if not impossible (see the discussion in Ref. [43]). This is often attributed to self-purification, the process whereby dopants are expelled from the NCs [44]. For example, several theoretical studies based on DFT calculations have shown that the lowest-energy position of a dopant is often at (near) the surface of the NCs [31,45–47]. The energy difference between core and surface sites can be of the order of 1 eV, but the situations depend strongly on the nature of the impurity and on the surface passivation (H, OH, SiO_2) [48–50]. The impurities placed on low-energy sites at the surface are often electrically inactive, for example in a form of tricoordinated P or B atoms [46–48].

On top of this, it was argued [43,51] that the doping process is not necessarily determined by the total energy of the impurities since it may be governed by kinetics rather than thermodynamics. In fact, it is instructive to consider a simple situation of a single impurity positioned in a NC containing $N = 1000$ core atoms (excluding surface) at thermal equilibrium. We assume that the impurity can be on any site with the same weight or can be placed on just one surface site where it is electrically inactive. If ΔE is the energy gain at the surface site compared to core sites, the probability to find the impurity in the core is close to zero [$\sim N \exp(-\Delta E)$] for ΔE of the order of 0.5 eV or above. In other words, doping of the NC is impossible except if the system is out-of-equilibrium (it must depend on the synthesis method), or if the dopants are stabilized in the NC core by the presence of the surrounding matrix [49,50].

Therefore, the conditions required to incorporate dopants into Si NCs are not really clarified by the theory. On the experimental side, the observation of ESR [8,52] and local surface plasmon resonance [21–23] demonstrates that electrically active impurities can be present in Si NCs. This is supported by APT experiments [14–18] showing that Si NCs can contain a non-negligible number of impurities. However, several works on doped Si NCs have shown that a large fraction of these impurities are electrically inactive [19–22,52], which suggests that many of them reside at the surface or in the surrounding matrix. This is confirmed by the observation of a strong reduction of the impurity concentration after HF etching of the NCs [52]. Coimplantation of Si and P (As) into SiO_2 samples was shown to be an efficient way to incorporate P or As impurities into Si NCs, as revealed by APT experiments [15]. However, coimplanted samples do not exhibit local surface plasmon resonance, suggesting that dopants are either compensated or inactive.

APT experiments [14–18] on matrices containing Si NCs show that the concentration of impurities is the highest in the regions where the NCs are located, with an accumulation at the interface region. Beyond this interface region, the results of APT experiments are more difficult to interpret, but it seems that the distribution profile into the Si NC core is approximately homogeneous. This is consistent with calculations on small Si NCs (diameter $\lesssim 2.2$ nm) showing a relatively weak dependence of the formation energy on the position of impurities placed in the NC core [45,46]. This dependence is expected to

be even weaker in NCs with larger size usually considered in experimental works.

High-resolution transmission electron microscopy (HRTEM) experiments combined with electron-energy-loss spectroscopy show that very large amounts of B and P are present in or on the surface of codoped colloidal Si NCs [26]. In the case of borophosphosilicate glass matrices, APT data reveal a B-rich layer surrounding the Si NCs, which could explain why codoped Si NCs disperse in polar solvents [17]. This experimental study reports the presence of individual P and B atoms in the NCs, but clusters of nearest-neighbor B-P atoms are also found. However, both HRTEM and APT experiments cannot give specific information on electrical-active dopants.

This survey of the literature shows that doping of Si NCs is not totally understood at the moment. In particular, it is possible that this process is not governed by thermodynamics. In this context, the concentration profile of electrically active dopants in the Si NCs is not precisely known. Therefore, in the present work, I consider configurations in which the impurities are placed at random positions, unless otherwise stated. I show in the next section that this hypothesis is supported by ESR experiments on P-doped Si NCs.

IV. HYPERFINE SPLITTING IN P-DOPED Si NCs

Before addressing the physics of codoped Si NCs, it is important to validate the methodology in the single-impurity case. However, doping NCs with a single impurity is very challenging. In addition, it is difficult to get detailed information on their electronic structure. In this context, ESR is a remarkable tool to probe the electronic states induced by dopants. This technique was used to study P donors in bulk Si [53]. The measurement of the hyperfine splitting $\Delta H_{\rm hfs}$ gives access to the wave function of the unpaired electron through its weight on the $3s$ orbital of the P atom. Remarkably, the hyperfine splitting was measured in Si NCs doped with a single P impurity [8]. The observed splitting was found to be much larger than in bulk and strongly dependent on the NC size. This behavior was interpreted by the strong confinement of the donor wave function. This interpretation was confirmed by *ab initio* pseudopotential calculations [54] even if these latter were limited to NC sizes much smaller than in experiments. As shown in the following, the tight-binding approach allows us to address much bigger NCs, including those that are commonly synthesized.

In the tight-binding model, the hyperfine splitting is written as [55]

$$\Delta H_{\rm hfs} = A\left|c_s^P\right|^2, \tag{2}$$

where c_s^P is the complex amplitude of the unpaired electron wave function on the s orbital of the P atom, and A is a constant that is deduced in the bulk Si limit where the calculation gives $|c_s^P|^2 = 7.9 \times 10^{-3}$ while a value for $\Delta H_{\rm hfs}$ of 42 G was measured [53].

The hyperfine splitting calculated in tight-binding is presented in Fig. 1(a) as a function of the NC diameter. In agreement with the experimental trends [8], $\Delta H_{\rm hfs}$ is strongly enhanced by the confinement. In the case of a P impurity placed at the center of the Si NCs, the calculated values

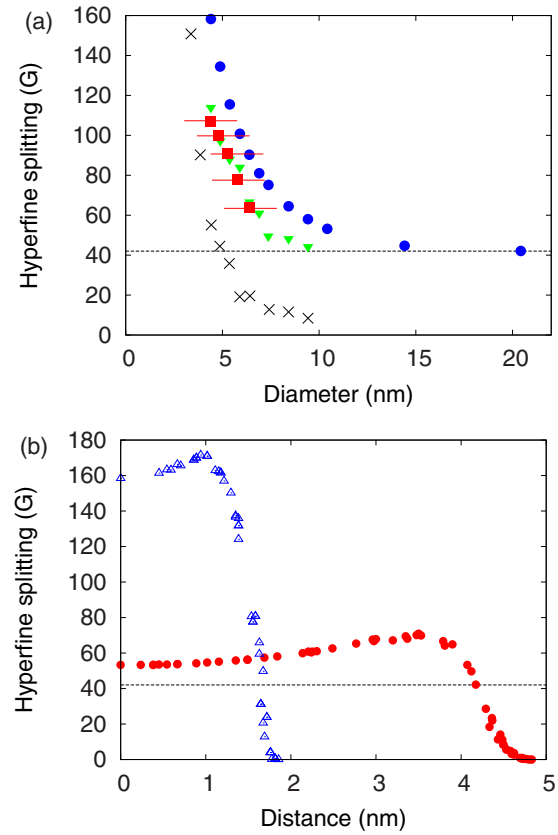

FIG. 1. (a) Hyperfine splitting $\Delta H_{\rm hfs}$ of ESR calculated for Si NCs doped with a single P impurity at the center (blue circles), or averaged over random positions of the dopant situated in the NC core (green triangles) or in a 1-nm-thick layer beneath the surface (black crosses), compared to the experimental values of Ref. [8] (red squares with horizontal error bars). (b) $\Delta H_{\rm hfs}$ vs distance of the P donor atom from the center of the Si NC, for a NC diameter of 4.4 nm (blue triangles) or 10.4 nm (red circles). In the two figures, the horizontal dashed line represents the experimental bulk value [53].

of $\Delta H_{\rm hfs}$ clearly overestimate the experimental data. On the contrary, if we assume that the impurity is situated in a thin shell (with a thickness of 1 nm) beneath the surface, the calculated values are far too small compared to experiments. Remarkably, if we consider a P donor placed at random positions, the agreement between theory and experiment is excellent. This shows that a uniform distribution of electrically active P impurities in Si NCs is a reasonable assumption. However, it is important to mention that ESR experiments do not exclude the presence of electrically inactive P impurities at the surface or close to the interface, even at high concentration.

These results can be understood from Fig. 1(b) showing that the hyperfine splitting has an important dependence on the position of the impurity in the NC due to the complex interplay between different phenomena. On the one hand, the quantum confinement tends to push the wave-function maximum at the center of the NC. On the other hand, the Coulomb potential tends to localize the electron close to the impurity nucleus [see Fig. 4(c) of Ref. [56]], but this Coulomb potential depends on the dopant position due to the dielectric

mismatch between the interior and the exterior of the NC. Its intensity tends to increase when the dopant gets closer to the surface due to the presence of positive polarization charges [38].

Figure 1(b) shows that, when the impurity nucleus approaches the surface, $\Delta H_{\rm hfs}$ becomes small because the maximum of the wave function is pushed far from the impurity site due to the strong confinement, which constrains the wave function to vanish at the surface. The competition between the opposite effects of the confinement and the Coulomb potential explains why $\Delta H_{\rm hfs}$ presents a maximum at an off-center position where the best compromise is found. In Fig. 1(a), $\Delta H_{\rm hfs}$ averaged over random dopant positions is reduced compared to its value at the NC center because of a geometrical effect, i.e., there are more atoms in the surface region than in the central one.

The results of Fig. 1(a) fully validate the tight-binding methodology for P donors in Si NCs. Unfortunately, there is no equivalent experimental data for B acceptors. However, since both B and P dopants behave as hydrogenic impurities in bulk Si, the present tight-binding model can be safely applied to both in Si NCs.

V. RESULTS FOR CODOPED Si NCs

A. Energy gap

The energy gap of Si NCs doped with one, two, five, or ten pairs of B-P dopants is shown in Fig. 2(a). In each case, I consider 40 configurations in which the position of each dopant is chosen randomly, avoiding surface sites. Compared to the undoped situation, the presence of a single B-P pair is sufficient to reduce the energy gap, in agreement with DFT calculations [31–34]. This reduction becomes considerably more important when the concentration of dopants is increased. In addition, the width of the energy gap varies from one random configuration to another, because the energy levels induced by the dopants depend on their respective position in the NC [32]. This variability, quantitatively assessed in Fig. 2(c), is not surprising since the Coulomb potential of an ensemble of point charges in a dielectric sphere depends on their spatial arrangement [38].

The mean value of the energy gap is presented in Fig. 2(b). In bulk Si, B and P doping introduces acceptor and donor energy levels in the gap, respectively. However, these energy levels are shallow [40], and therefore the reduction of the gap is relatively small. The influence of doping on the electronic structure of Si NCs is much more important. Even a single pair of B-P atoms leads to a gap narrowing of the order of hundreds of meV. This is mainly due to the so-called dielectric confinement effect coming from the dielectric mismatch between the Si NC and its environment, the latter being characterized by a dielectric constant usually much smaller than in Si. When point charges are placed inside a Si NC, Coulomb interactions are partially unscreened because some polarization charges remain at the surface, whereas in bulk Si they are pushed at infinity [38]. As a consequence, single dopants are characterized by deeper energy levels in the energy gap [56,57]. A similar effect takes place in Si nanowires [41]. However, in NCs doped with the same number of donors and acceptors, this dielectric confinement effect is reduced compared to the single dopant case because the total polarization charge integrated on the NC surface is equal to zero.

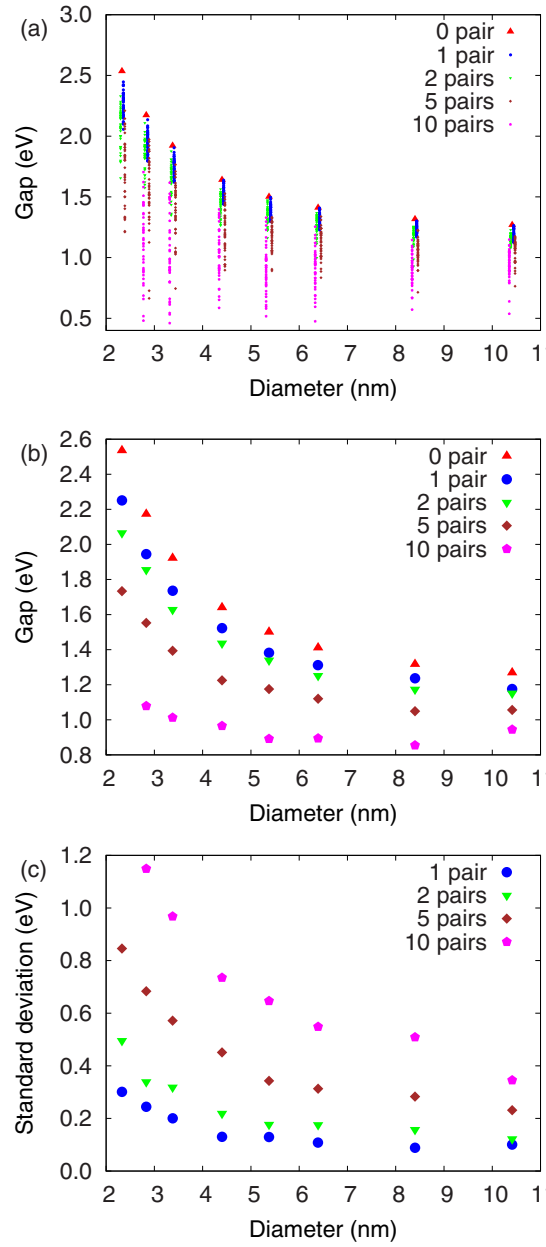

FIG. 2. (a) Single-particle energy gap of undoped Si NCs (red triangles) compared to codoped NCs (one B-P pair, blue circles; two pairs, green triangles; five pairs, brown lozenges; ten pairs, magenta pentagons). For codoped NCs, 40 random configurations of impurity positions are considered. (b) Mean value of the single-particle energy gaps taken over the 40 configurations. (c) Standard deviation of the energy gaps with respect to the mean value.

The mean energy gap continues to decrease when additional B-P pairs are added to the NCs [Fig. 2(b)] and it becomes quite small in the case of 10 B-P pairs. However, the effect of the ten pairs becomes slightly less important for NC diameters above ∼10 nm. In that case, the distance between dopants increases and their mutual influence decreases.

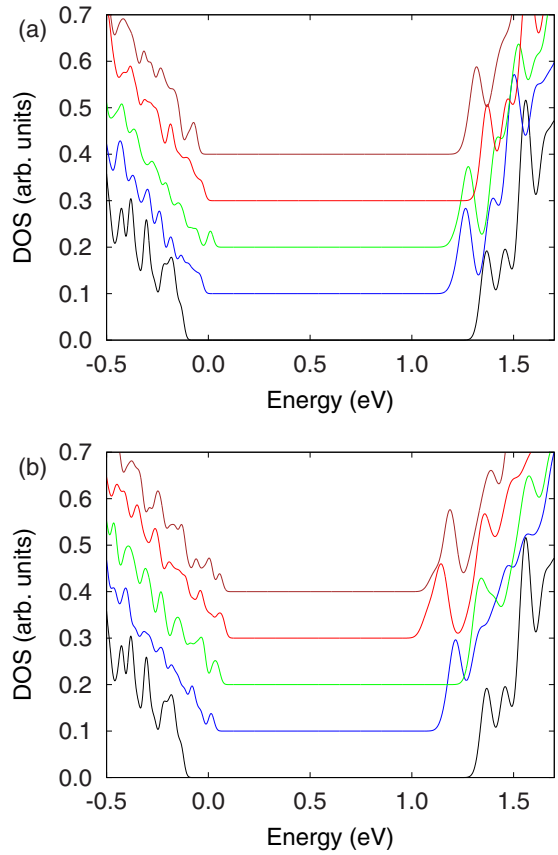

FIG. 3. Single-particle DOS calculated for a NC diameter of 5.4 nm. The lowest curve in black is calculated for the undoped NC, and the other colored curves are obtained for different configurations of NCs doped with two (a) or five (b) B-P pairs.

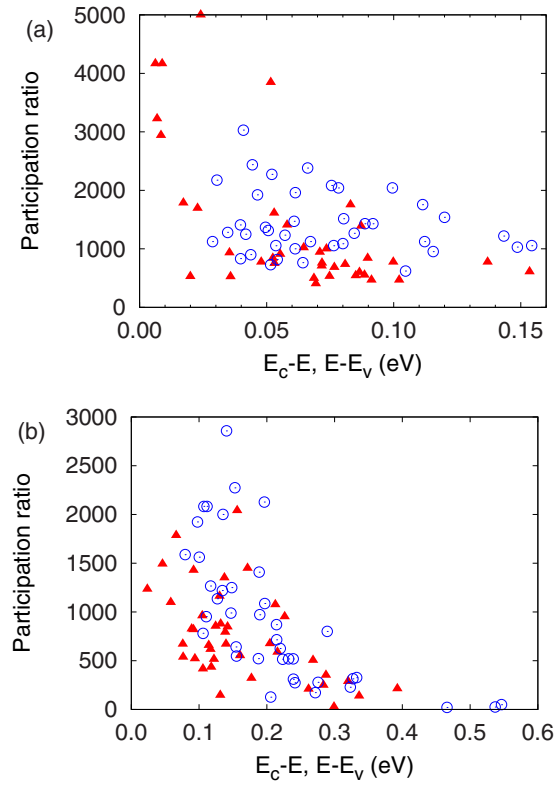

FIG. 4. Participation ratio χ calculated for the lowest conduction state (red triangles) and the highest valence state (blue circles) of Si NCs doped with two (a) or ten (b) B-P pairs [NC diameter = 8.4 nm]. The results are obtained for 40 random configurations of impurity positions and are presented vs the depth of the energy level into the gap, i.e., the difference between the energy E of the state and its value in the undoped NC (E_c for a conduction state, E_v for a valence state).

B. Density of states

It is also enlightening to look at the single-particle density of states (DOS). In Fig. 3, we consider different situations of codoped NCs. Even if there are important variations from one situation to another, the comparison with the DOS calculated for the undoped NC reveals clear trends. In each case, the codoping brings peaks in the energy gap of the pristine NC. The resulting band-gap narrowing is, on average, almost equally shared between the two sides of the gap. Remarkably, a very similar behavior is found when the NCs are doped with two or five B-P pairs, only the amplitude of the gap narrowing increases with the number of dopants. All these results are qualitatively in excellent agreement with the recent measurements of the DOS performed on codoped Si NCs using STS [35], even if it is not possible to make direct comparisons between theoretical and experimental spectra since both the number of dopants and their spatial localization are not known. However, a quantitative analysis of the STS gaps will be presented in Sec. VI.

C. Localization of states

It is also important to characterize the effect of the codoping on the wave functions at the gap edges, in particular on their spatial localization. A convenient probe of this localization is the participation ratio χ defined for each state as $\chi = [\sum_i (\sum_\alpha |c_{i\alpha}|^2)^2]^{-1}$, where $c_{i\alpha}$ is the complex amplitude of the wave function on the site (atom) i and orbital α. χ measures the number of sites that contribute to the state.

Results for NCs of 8.4 nm diameter containing 15 498 Si atoms are presented in Fig. 4 for different configurations of codoping. In the presence of two B-P pairs per NC, Fig. 4(a) shows that χ is always between 400 and 5000, meaning that the band-edge states remain substantially delocalized. Even if χ is characterized by quite scattered values, it tends to decrease when the energy level goes deeper into the gap, which is the expected behavior found, for example, in amorphous Si [58]. These trends are accentuated in the case of NCs doped with 10 B-P pairs [Fig. 4(b)] where there are situations characterized by deep levels and very localized wave functions. However, there are still many configurations of doping where the localization of the wave functions is not too strong ($\chi > 500$).

D. Dopants at the surface

Figure 5 presents the mean energy gap of Si NCs doped with two B-P pairs. Two situations are compared. First, all dopants

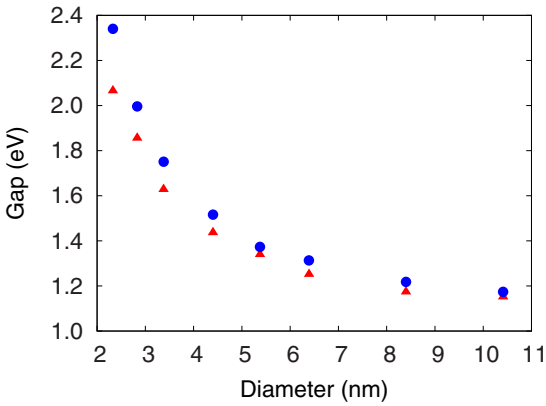

FIG. 5. Red triangles: single-particle energy gap of NCs codoped with two B-P pairs calculated as an average value over 40 random configurations of impurity positions. Blue circles: same but the two P impurities are placed at the surface.

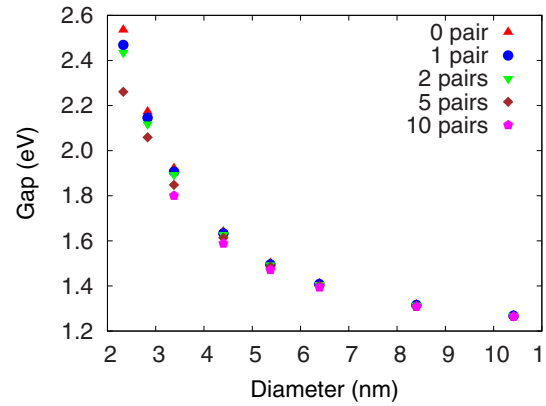

FIG. 6. Single-particle energy gap of undoped Si NCs (red triangles) compared to codoped NCs (one B-P cluster, blue circles; two clusters, green triangles; five clusters, brown lozenges; ten clusters, magenta pentagons). For codoped NCs, the B and P atoms of each cluster are at nearest-neighbor positions, and 40 random configurations of cluster positions are considered.

are placed at random positions, but surface sites are excluded [same data as in Fig. 2(b)]. Second, the two P atoms of the pairs are placed at surface sites chosen randomly. It is assumed that the P atoms are still characterized by a fourfold coordination (in reality, this is often not the case), i.e., they are still acting as donor impurities characterized by a charge $+e$ at their nucleus. Figure 5 shows that the energy gaps in the two situations are quite similar; the differences become visible only for diameters smaller than 5 nm. However, even in those cases, the increase of the energy gap due to the confinement is largely preserved, and the corrections induced by the different positions of the dopants remain relatively small. Very similar results are obtained when the B atoms instead of the P atoms are placed at the surface (not shown).

E. Nearest-neighbor B-P clusters

As already mentioned in Sec. III, APT experiments on borophosphosilicate glass matrices reveal that codoped Si NCs also contain clusters of nearest-neighbor B-P atoms, in addition to individual impurities [17] (hereafter, a B-P cluster refers to a pair of nearest-neighbor B-P impurities). This raises the question of their role in the NC gap. Figure 6 presents the energy gap of Si NCs doped with B-P clusters. Except for the smallest sizes, the presence of B-P clusters has almost no effect on the gap. This is due to the very weak Coulomb potential induced by each cluster characterized by a zero total charge. More generally, the influence of a B-P pair on the energy gap decreases when the distance between the two atoms is reduced [33].

VI. COMPARISON WITH EXPERIMENTS AND DISCUSSION

Experimental and theoretical data on codoped Si NCs are presented together in Fig. 7. To compare with photoluminescence (PL) peak positions measured on codoped Si NCs [26], the optical gaps have been calculated by applying excitonic corrections to the single-particle gaps [Fig. 7(a)]. To avoid heavy calculations on too many configurations, I consider that the excitonic correction on the mean energy gap is the same as in undoped Si NCs [59]. This approximation is reasonable because excitonic corrections are dominated by polarization-charge (or image-charge) effects [38,59], which, after averaging over random positions of the dopants, should be close to the pristine case. Figure 7(a) shows that the PL peak energies for NCs in a colloidal solution are compatible with the theoretical results for a small number of randomly placed B-P pairs, typically between two and five, plus possibly an unknown number of nearest-neighbor B-P clusters that do not change the NC gap. The PL peaks measured in a borophosphosilicate glass matrix are at lower energy [26], for reasons that are not totally clear at the moment. In that case, the PL peak energies would be compatible with the calculated ones for a larger number of B-P pairs, between five and ten. A possible explanation for this difference could be found in the chemical treatment needed to make NC colloidal solutions from glass matrices, which could remove a certain number of B-P pairs located at (near) the NC surface.

In agreement with the experiments, the calculations show that a PL emission below the band gap of bulk Si is possible, even for a small number ($\sim$5) of B-P pairs in NCs with a sufficiently large diameter. In spite of the redshift of the PL emission induced by the codoping, the theory predicts an important dependence of the emission energy on the NC size (for a number of pairs below five), in quantitative agreement with the experimental trends. As shown in Sec. V C, the wave functions at the band edges are not too strongly localized by the Coulomb potential of the dopants, and therefore they are still sensitive to quantum-confinement effects. Interestingly, this behavior, in which (partial) localization and quantum confinement effects are mutually present, was also found in clusters of amorphous silicon [60].

The gap of codoped Si NCs was also measured in STS [35]. In Fig. 7(b), the theoretical data presented for comparison are the single-particle gaps, since STS experiments probe

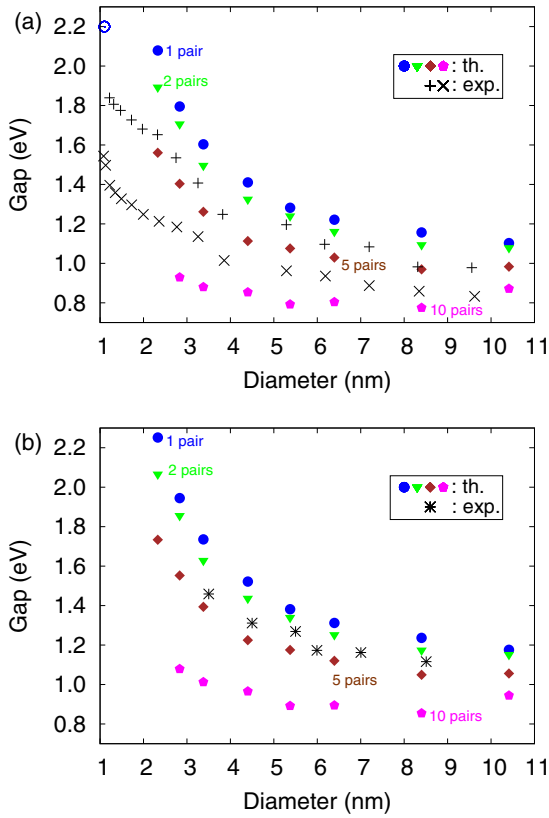

FIG. 7. Theoretical (th.) energy gaps for one B-P pair (blue circles), two pairs (green triangles), five pairs (brown lozenges), and ten pairs (magenta pentagons) compared to experimental (exp.) data. (a) Theory, excitonic gaps. Experiments, PL peak positions measured on codoped Si NCs in a colloidal solution (+) or in a borophosphosilicate glass matrix (×) [26]. (b) Theory, single-particle energy gaps. Experiments, gaps measured by STS [35].

single-particle excitations.[1] Once again, the measured gaps are compatible with the calculated ones for a number of randomly placed B-P pairs, between two and five. In that cases, the calculated DOS are also in qualitative agreement with STS spectra (Sec. V B).

APT experiments on codoped Si NCs in borophosphosilicate glass give concentrations of about 1.5% for B and 4% for P [17]. For a NC of 3.4 nm diameter containing ∼700 Si atoms, this corresponds to ∼10 B and ∼28 P impurities. Even larger numbers (100–1000) of impurities were reported in Ref. [28]. The present work suggests that many of these impurities are electrically inactive, or they are in the form of nearest-neighbor B-P clusters. The fact that many impurities are electrically inactive is not yet understood but is confirmed by other studies [19–22,52]. New experimental studies are clearly needed to determine the electrical activity of the large number of impurities present at NC surfaces or in their vicinity.

All calculations in the present work are based on the hypothesis of an equal number of donor and acceptor impurities, which, at first glance, would appear unlikely. However, this exact compensation is clearly demonstrated by STS measurements showing that the Fermi level lies approximately at the middle of the NC energy gap [35]. This surprising situation could be explained by the small formation energy for simultaneous B and P doping [32].

VII. CONCLUSION

Tight-binding calculations of the electronic structure of Si NCs doped with the same number of B and P impurities have been presented. They show that the experimental data based on optical and electrical spectroscopy could be explained by configurations where the Si NCs contain a small number ($\lesssim$5) of B-P pairs. The presence of these codopants placed at random positions tends to reduce the energy gap of the NCs even if quantum confinement effects remain visible. The observation of PL emission below the band gap of bulk Si is supported by the theory. However, the comparison with experiments suggests that many impurities in codoped Si NCs are electrically inactive. These impurities could be at the surface or in the form of B-P clusters since the present calculations show that B and P impurities placed at nearest-neighbor positions have a weak influence on the NC energy gap. This work confirms that codoped Si NCs are very interesting systems, not only for fundamental studies but also for future applications of Si photonics.

[1] In principle, STS gaps should be corrected to account for small self-capacitance effects, of the order of ∼0.1 eV.

[1] L. T. Canham, Appl. Phys. Lett. **57**, 1046 (1990).
[2] F. Priolo, T. Gregorkiewicz, M. Galli, and T. F. Krauss, Nat. Nano **9**, 19 (2014).
[3] C. M. Hessel, D. Reid, M. G. Panthani, M. R. Rasch, B. W. Goodfellow, J. Wei, H. Fujii, V. Akhavan, and B. A. Korgel, Chem. Mater. **24**, 393 (2012).
[4] M. L. Mastronardi, F. Maier-Flaig, D. Faulkner, E. J. Henderson, C. Kübel, U. Lemmer, and G. A. Ozin, Nano Lett. **12**, 337 (2012).
[5] J. B. Miller, A. R. Van Sickle, R. J. Anthony, D. M. Kroll, U. R. Kortshagen, and E. K. Hobbie, ACS Nano **6**, 7389 (2012).
[6] M. Fujii, S. Hayashi, and K. Yamamoto, J. Appl. Phys. **83**, 7953 (1998).
[7] A. Mimura, M. Fujii, S. Hayashi, D. Kovalev, and F. Koch, Phys. Rev. B **62**, 12625 (2000).
[8] M. Fujii, A. Mimura, S. Hayashi, Y. Yamamoto, and K. Murakami, Phys. Rev. Lett. **89**, 206805 (2002).
[9] M. Fujii, K. Toshikiyo, Y. Takase, Y. Yamaguchi, and S. Hayashi, J. Appl. Phys. **94**, 1990 (2003).
[10] K. Sato, N. Fukata, and K. Hirakuri, Appl. Phys. Lett. **94**, 161902 (2009).
[11] M. Perego, C. Bonafos, and M. Fanciulli, Nanotechnology **21**, 025602 (2010).
[12] S. Kim, S. H. Hong, J. H. Park, D. Y. Shin, D. H. Shin, S.-H. Choi, and K. J. Kim, Nanotechnology **22**, 275205 (2011).

[13] H. Sugimoto, M. Fujii, M. Fukuda, K. Imakita, and S. Hayashi, J. Appl. Phys. **110**, 063528 (2011).
[14] S. Gutsch, A. M. Hartel, D. Hiller, N. Zakharov, P. Werner, and M. Zacharias, Appl. Phys. Lett. **100**, 233115 (2012).
[15] R. Khelifi, D. Mathiot, R. Gupta, D. Muller, M. Roussel, and S. Duguay, Appl. Phys. Lett. **102**, 013116 (2013).
[16] H. Gnaser, S. Gutsch, M. Wahl, R. Schiller, M. Kopnarski, D. Hiller, and M. Zacharias, J. Appl. Phys. **115**, 034304 (2014).
[17] K. Nomoto, H. Sugimoto, A. Breen, A. V. Ceguerra, T. Kanno, S. P. Ringer, I. P. Wurfl, G. Conibeer, and M. Fujii, J. Phys. Chem. C **120**, 17845 (2016).
[18] K. Nomoto, D. Hiller, S. Gutsch, A. V. Ceguerra, A. Breen, M. Zacharias, G. Conibeer, I. Perez-Wurfl, and S. P. Ringer, Phys. Status Solidi RRL **11**, 1600376 (2016).
[19] X. D. Pi, R. Gresback, R. W. Liptak, S. A. Campbell, and U. Kortshagen, Appl. Phys. Lett. **92**, 123102 (2008).
[20] D. Hiller, J. López-Vidrier, S. Gutsch, M. Zacharias, M. Wahl, W. Bock, A. Brodyanski, M. Kopnarski, K. Nomoto, J. Valenta, and D. König, Sci. Rep. **7**, 8337 (2017).
[21] D. J. Rowe, J. S. Jeong, K. A. Mkhoyan, and U. R. Kortshagen, Nano Lett. **13**, 1317 (2013).
[22] S. Zhou, X. Pi, Z. Ni, Y. Ding, Y. Jiang, C. Jin, C. Delerue, D. Yang, and T. Nozaki, ACS Nano **9**, 378 (2015).
[23] N. J. Kramer, K. S. Schramke, and U. R. Kortshagen, Nano Lett. **15**, 5597 (2015).
[24] M. Fujii, Y. Yamaguchi, Y. Takase, K. Ninomiya, and S. Hayashi, Appl. Phys. Lett. **85**, 1158 (2004).
[25] M. Fukuda, M. Fujii, and S. Hayashi, J. Lumin. **131**, 1066 (2011).
[26] H. Sugimoto, M. Fujii, K. Imakita, S. Hayashi, and K. Akamatsu, J. Phys. Chem. C **116**, 17969 (2012).
[27] T. Nakamura, S. Adachi, M. Fujii, K. Miura, and S. Yamamoto, Phys. Rev. B **85**, 045441 (2012).
[28] H. Sugimoto, M. Fujii, K. Imakita, S. Hayashi, and K. Akamatsu, J. Phys. Chem. C **117**, 6807 (2013).
[29] H. Sugimoto, M. Fujii, K. Imakita, S. Hayashi, and K. Akamatsu, J. Phys. Chem. C **117**, 11850 (2013).
[30] Y. Hori, S. Kano, H. Sugimoto, K. Imakita, and M. Fujii, Nano Lett. **16**, 2615 (2016).
[31] S. Ossicini, E. Degoli, F. Iori, E. Luppi, R. Magri, G. Cantele, F. Trani, and D. Ninno, Appl. Phys. Lett. **87**, 173120 (2005).
[32] F. Iori, E. Degoli, R. Magri, I. Marri, G. Cantele, D. Ninno, F. Trani, O. Pulci, and S. Ossicini, Phys. Rev. B **76**, 085302 (2007).
[33] F. Iori, E. Degoli, M. Palummo, and S. Ossicini, Superlattices Microstruct. **44**, 337 (2008).
[34] F. Iori and S. Ossicini, Physica E **41**, 939 (2009).
[35] O. Ashkenazi, D. Azulay, I. Balberg, S. Kano, H. Sugimoto, M. Fujii, and O. Millo, Nanoscale **9**, 17884 (2017).
[36] C. Delerue, M. Lannoo, G. Allan, E. Martin, I. Mihalcescu, J. C. Vial, R. Romestain, F. Muller, and A. Bsiesy, Phys. Rev. Lett. **75**, 2228 (1995).
[37] Y. M. Niquet, C. Delerue, G. Allan, and M. Lannoo, Phys. Rev. B **62**, 5109 (2000).
[38] C. Delerue and M. Lannoo, *Nanostructures: Theory and Modeling* (Springer, Berlin, 2004).
[39] C. Delerue, M. Lannoo, and G. Allan, Phys. Rev. B **68**, 115411 (2003).
[40] W. Kohn and J. M. Luttinger, Phys. Rev. **98**, 915 (1955).
[41] M. Diarra, Y.-M. Niquet, C. Delerue, and G. Allan, Phys. Rev. B **75**, 045301 (2007).
[42] J. Mansir, P. Conti, Z. Zeng, J. J. Pla, P. Bertet, M. W. Swift, C. G. Van de Walle, M. L. W. Thewalt, B. Sklenard, Y. M. Niquet, and J. J. L. Morton, Phys. Rev. Lett. **120**, 167701 (2018).
[43] S. C. Erwin, L. Zu, M. I. Haftel, A. L. Efros, T. A. Kennedy, and D. J. Norris, Nature (London) **436**, 91 (2005).
[44] G. M. Dalpian and J. R. Chelikowsky, Phys. Rev. Lett. **96**, 226802 (2006).
[45] G. Cantele, E. Degoli, E. Luppi, R. Magri, D. Ninno, G. Iadonisi, and S. Ossicini, Phys. Rev. B **72**, 113303 (2005).
[46] X. Pi, X. Chen, and D. Yang, J. Phys. Chem. C **115**, 9838 (2011).
[47] X. Chen, X. Pi, and D. Yang, J. Phys. Chem. C **115**, 661 (2011).
[48] A. Carvalho, B. Celikkol, J. Coutinho, and P. R. Briddon, J. Phys.: Conf. Ser. **281**, 012027 (2011).
[49] C. Alexandra, O. Sven, B. Manuel, R. M. J., and B. Patrick, Phys. Status Solidi A **209**, 1847 (2012).
[50] R. Guerra and S. Ossicini, J. Am. Chem. Soc. **136**, 4404 (2014).
[51] M.-H. Du, S. C. Erwin, A. L. Efros, and D. J. Norris, Phys. Rev. Lett. **100**, 179702 (2008).
[52] A. R. Stegner, R. N. Pereira, R. Lechner, K. Klein, H. Wiggers, M. Stutzmann, and M. S. Brandt, Phys. Rev. B **80**, 165326 (2009).
[53] G. Feher, Phys. Rev. **114**, 1219 (1959).
[54] D. V. Melnikov and J. R. Chelikowsky, Phys. Rev. Lett. **92**, 046802 (2004).
[55] C. Slichter, *Principles of Magnetic Resonance*, Springer Series in Solid-State Sciences (Springer, Berlin, 1996).
[56] G. Allan, C. Delerue, M. Lannoo, and E. Martin, Phys. Rev. B **52**, 11982 (1995).
[57] M. Lannoo, C. Delerue, and G. Allan, Phys. Rev. Lett. **74**, 3415 (1995).
[58] G. Allan, C. Delerue, and M. Lannoo, Phys. Rev. B **57**, 6933 (1998).
[59] C. Delerue, M. Lannoo, and G. Allan, Phys. Rev. Lett. **84**, 2457 (2000).
[60] G. Allan, C. Delerue, and M. Lannoo, Phys. Rev. Lett. **78**, 3161 (1997).